A bright megaelectronvolt emission line in γ-ray burst GRB 221009A

arXiv: 2303.16223

Maria Edvige Ravasio, Om Sharan Salafia, Gor Oganesyan, Alessio Mei, Giancarlo Ghirlanda, Stefano Ascenzi, Biswajit Banerjee, Samanta Macera, Marica Branchesi, Peter G. Jonker, Andrew Levan, Daniele Bjørn Malesani, Katharine B. Mulrey, Andrea Giuliani, Annalisa Celotti and Gabriele Ghisellini

Alessandro Armando Vigliano:
viglianoalessandro@gmail.com

Abstract

The highly variable and energetic pulsed emission of a long gamma–ray burst (GRB) is thought to originate from local, rapid dissipation of kinetic or magnetic energy within an ultra-relativistic jet launched by a newborn compact object, formed during the collapse of a massive star. The spectra of GRB pulses are best modelled by power-law segments, indicating the dominance of non-thermal radiation processes. Spectral lines in the X-ray and soft γ-ray regime for the afterglow have been searched for intensively, but never confirmed. No line features ever been identified in the high energy prompt emission. Here we report the discovery of a highly significant ($> 6\sigma$) narrow emission feature at around 10 MeV in the brightest ever GRB 221009A. By modelling its profile with a Gaussian, we find a roughly constant width $\sigma \sim 1$ MeV and temporal evolution both in energy (~ 12 MeV to ~ 6 MeV) and luminosity ($\sim 10^{50}$ erg/s to $\sim 2 \times 10^{49}$ erg/s) over 80 seconds. We interpret this feature as a blue-shifted annihilation line of relatively cold ($k_{\mathrm{B}}T \ll m_{\mathrm{e}}c^2$) electron-positron pairs, which could have formed within the jet region where the brightest pulses of the GRB were produced. A detailed understanding of the conditions that can give rise to such a feature could shed light on the so far poorly understood GRB jet properties and energy dissipation mechanism.

Abstract

The highly variable and energetic pulsed emission of a long gamma–ray burst (GRB) is thought to originate from local, rapid dissipation of kinetic or magnetic energy within an ultra-relativistic jet launched by a newborn compact object, formed during the collapse of a massive star. The spectra of GRB pulses are best modelled by power-law segments, indicating the dominance of non-thermal radiation processes. Spectral lines in the X-ray and soft γ-ray regime for the afterglow have been searched for intensively, but never confirmed. No line features ever been identified in the high energy prompt emission. Here we report the discovery of a highly significant ($> 6\sigma$) narrow emission feature at around 10 MeV in the brightest ever GRB 221009A. By modelling its profile with a Gaussian, we find a roughly constant width $\sigma \sim 1$ MeV and temporal evolution both in energy (~ 12 MeV to ~ 6 MeV) and luminosity ($\sim 10^{50}$ erg/s to $\sim 2 \times 10^{49}$ erg/s) over 80 seconds. We interpret this feature as a blue-shifted annihilation line of relatively cold ($k_{\mathrm{B}}T \ll m_{\mathrm{e}}c^2$) electron-positron pairs, which could have formed within the jet region where the brightest pulses of the GRB were produced. A detailed understanding of the conditions that can give rise to such a feature could shed light on the so far poorly understood GRB jet properties and energy dissipation mechanism.

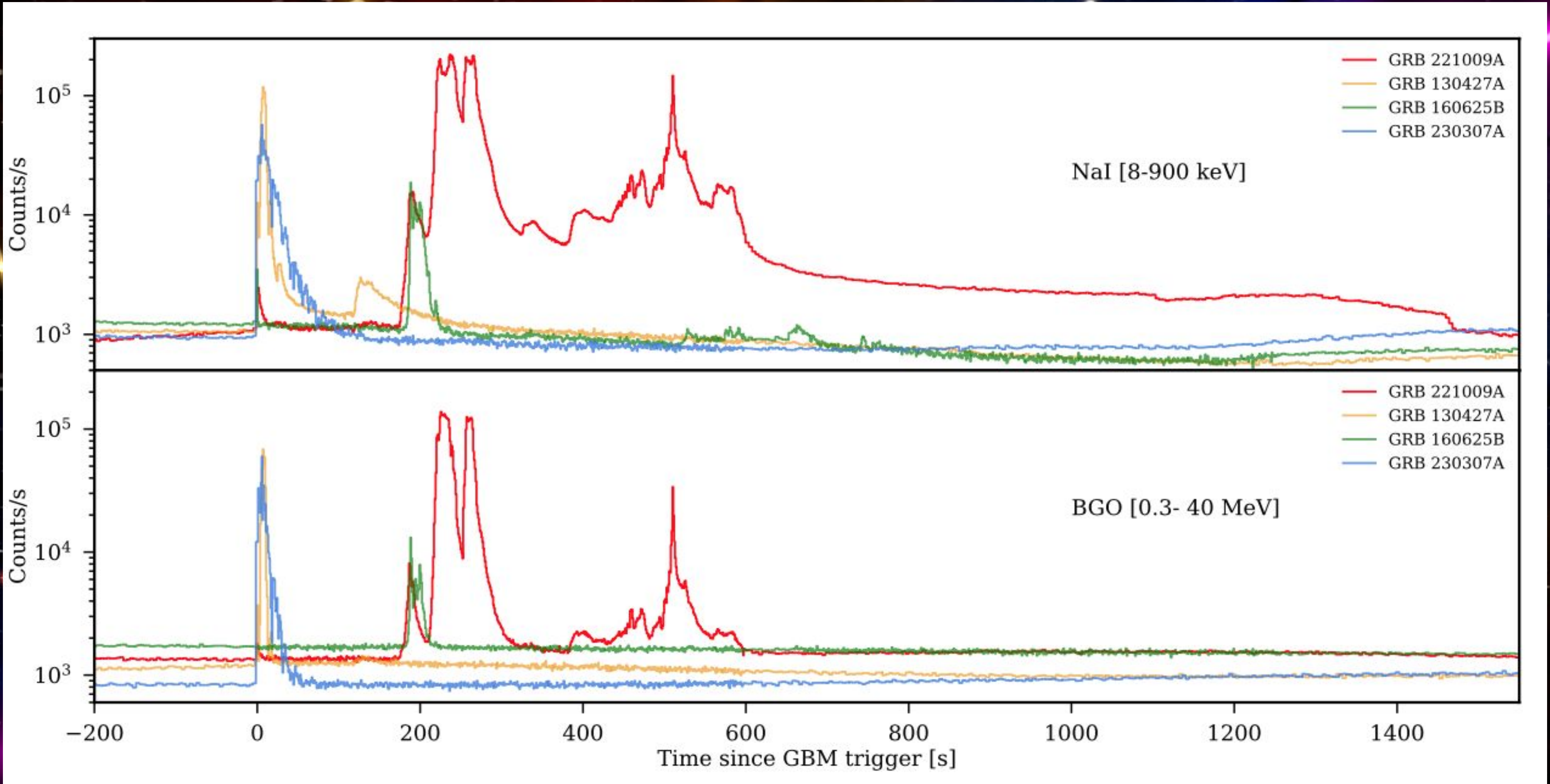

GRB 221009A
GRB 130427A
GRB 160625B
GRB 230307A
NaI [8-900 keV]
Counts/s
BGO [0.3- 40 MeV]
Time since GBM trigger [s]

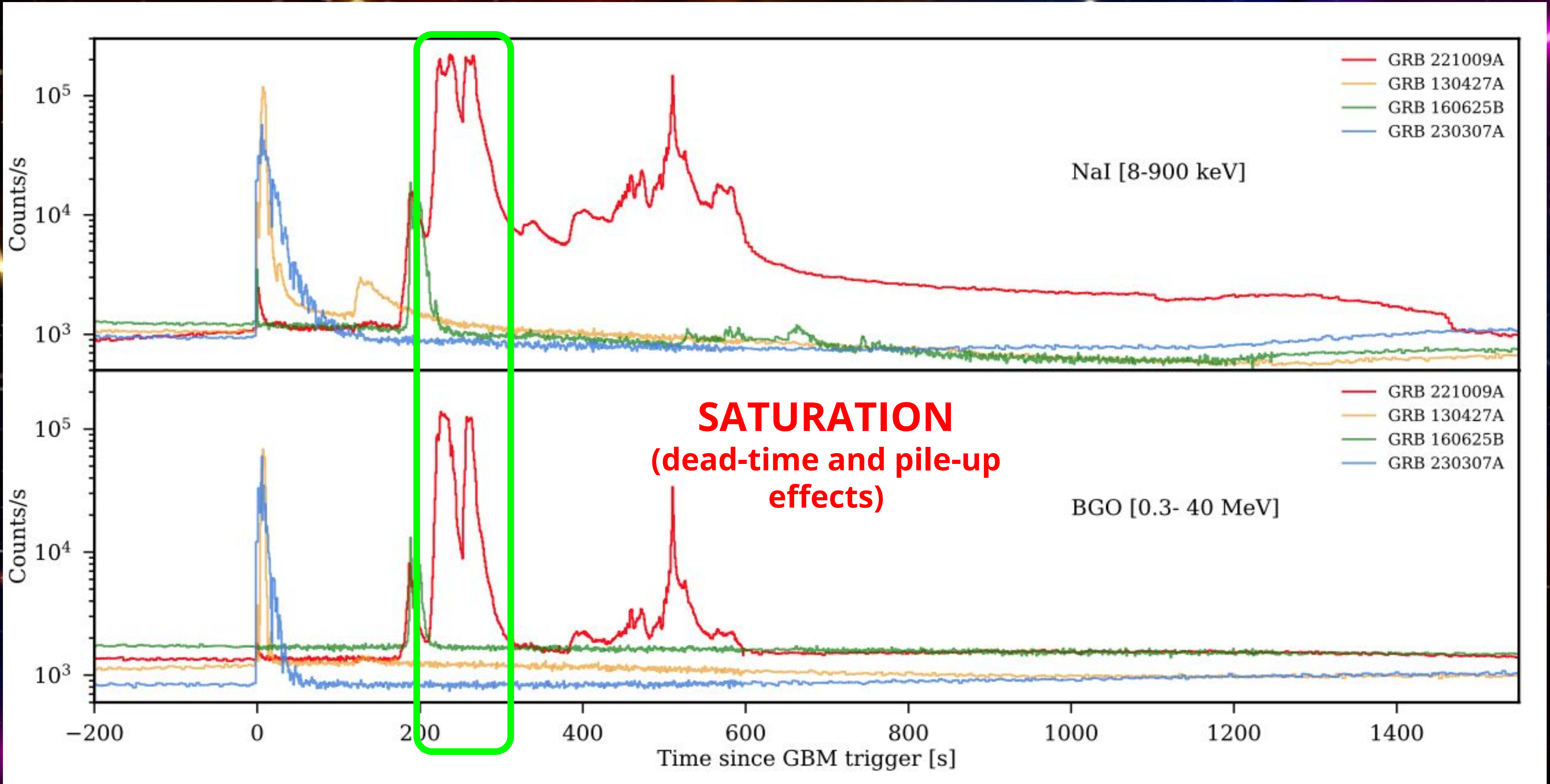
GRB 221009A
GRB 130427A
GRB 160625B
GRB 230307A
NaI [8-900 keV]
Counts/s
SATURATION
(dead-time and pile-up effects)
BGO [0.3- 40 MeV]
Time since GBM trigger [s]

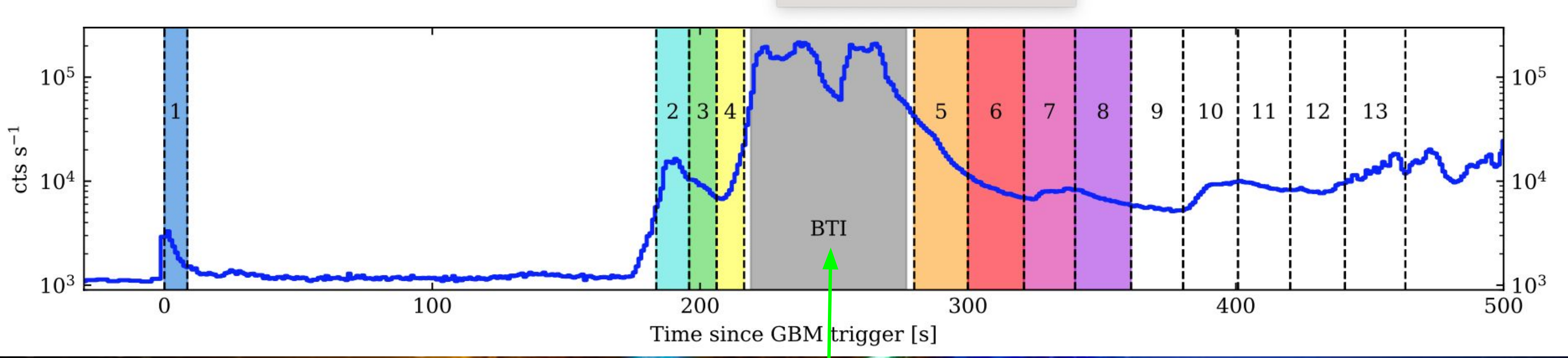

SATURATION

219-277 s Bad Time Interval

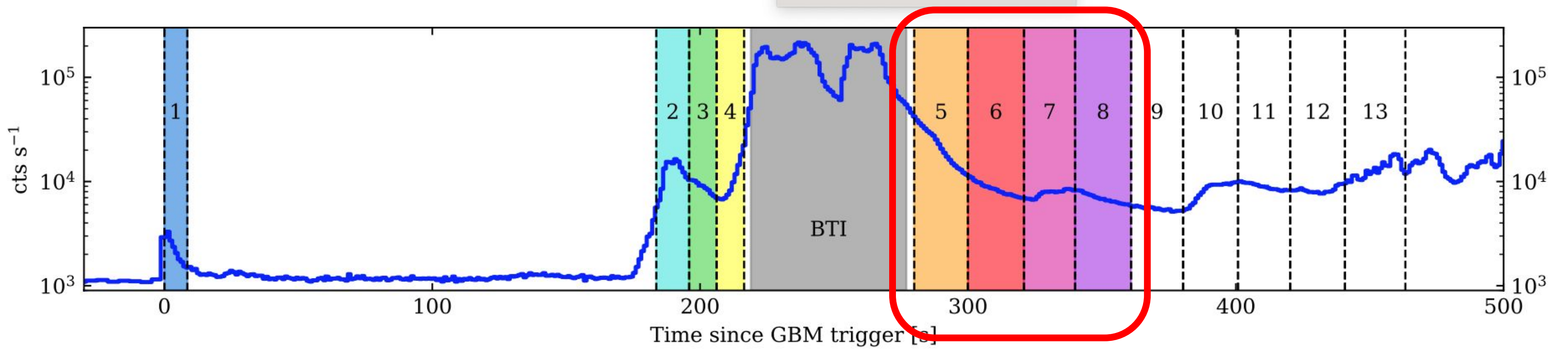

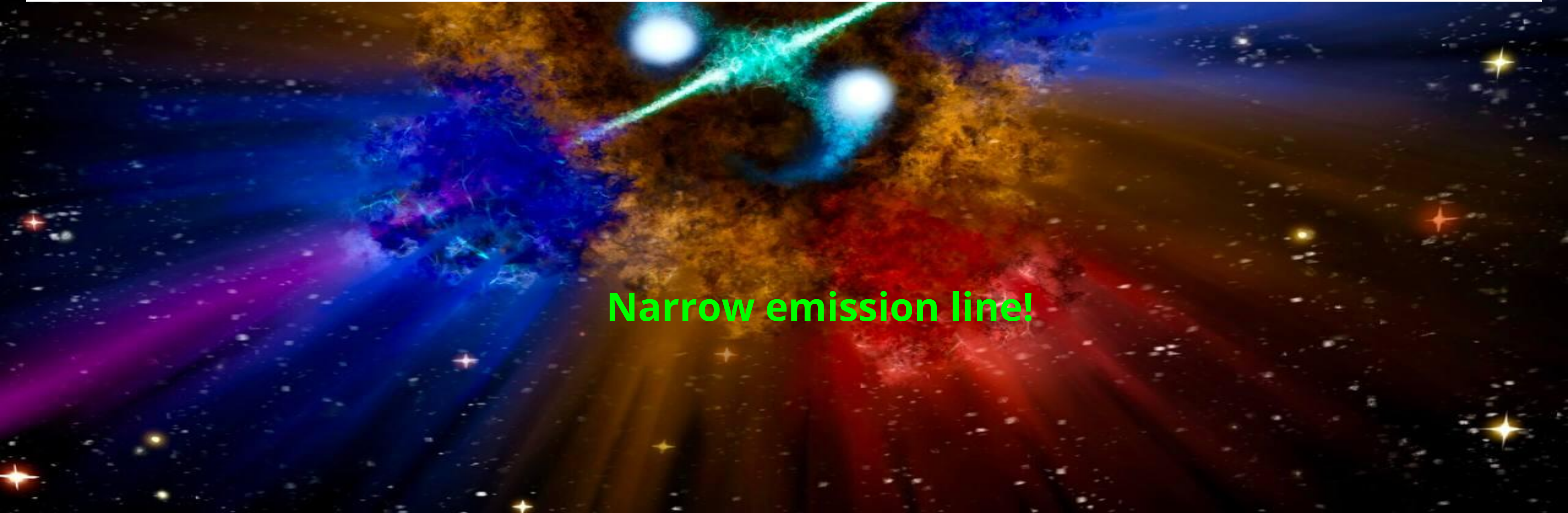

Narrow emission line!

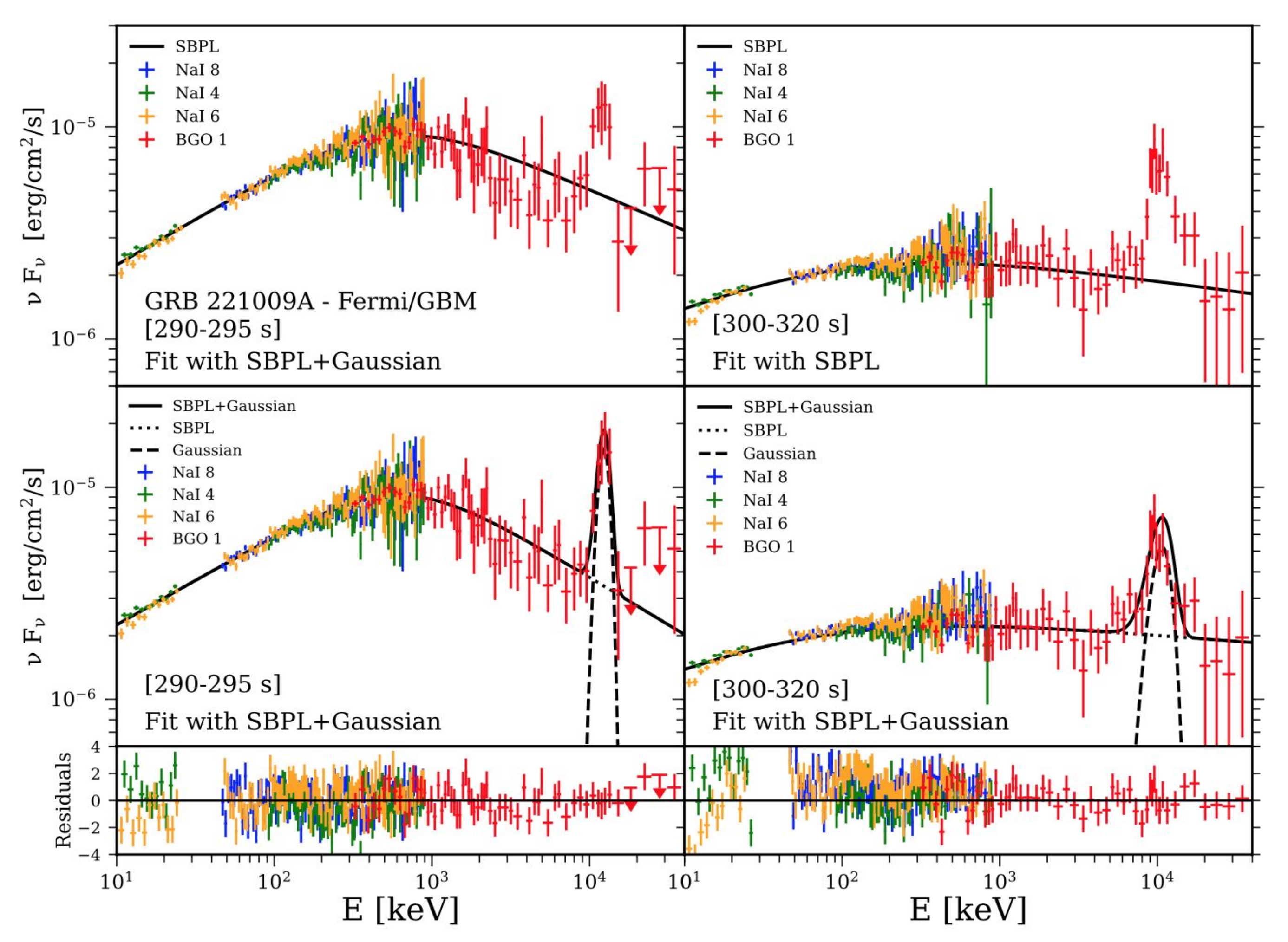

GRB 221009A - Fermi/GBM
[290-295 s]
Fit with SBPL+Gaussian
[300-320 s]
Fit with SBPL
[290-295 s]
Fit with SBPL+Gaussian
[300-320 s]
Fit with SBPL+Gaussian
SBPL
SBPL+Gaussian
Gaussian
NaI 8
NaI 4
NaI 6
BGO 1
ν F_ν [erg/cm²/s]
Residuals
E [keV]

Akaike Information Criterion

- Method for evaluating and comparing statistical models
- Provides a measure of the quality of the estimate of a statistical model by taking into account both the goodness of fit and the complexity of the model

$$\mathrm{AIC} = 2k - 2\ln(\hat{L})$$

- k = number of parameters, L = maximized likelihood of the model
- Models with lower AIC are favoured

Akaike Information Criterion

- Method for evaluating and comparing statistical models
- Provides a measure of the quality of the estimate of a statistical model by taking into account both the goodness of fit and the complexity of the model

$$\mathrm{AIC} = 2k - 2\ln(\hat{L})$$

- k = number of parameters, L = maximized likelihood of the model
- Models with lower AIC are favoured

ΔAIC = 49 (280-300s)**, 141** (300-320s) **!!**
(without-with) Gaussian component

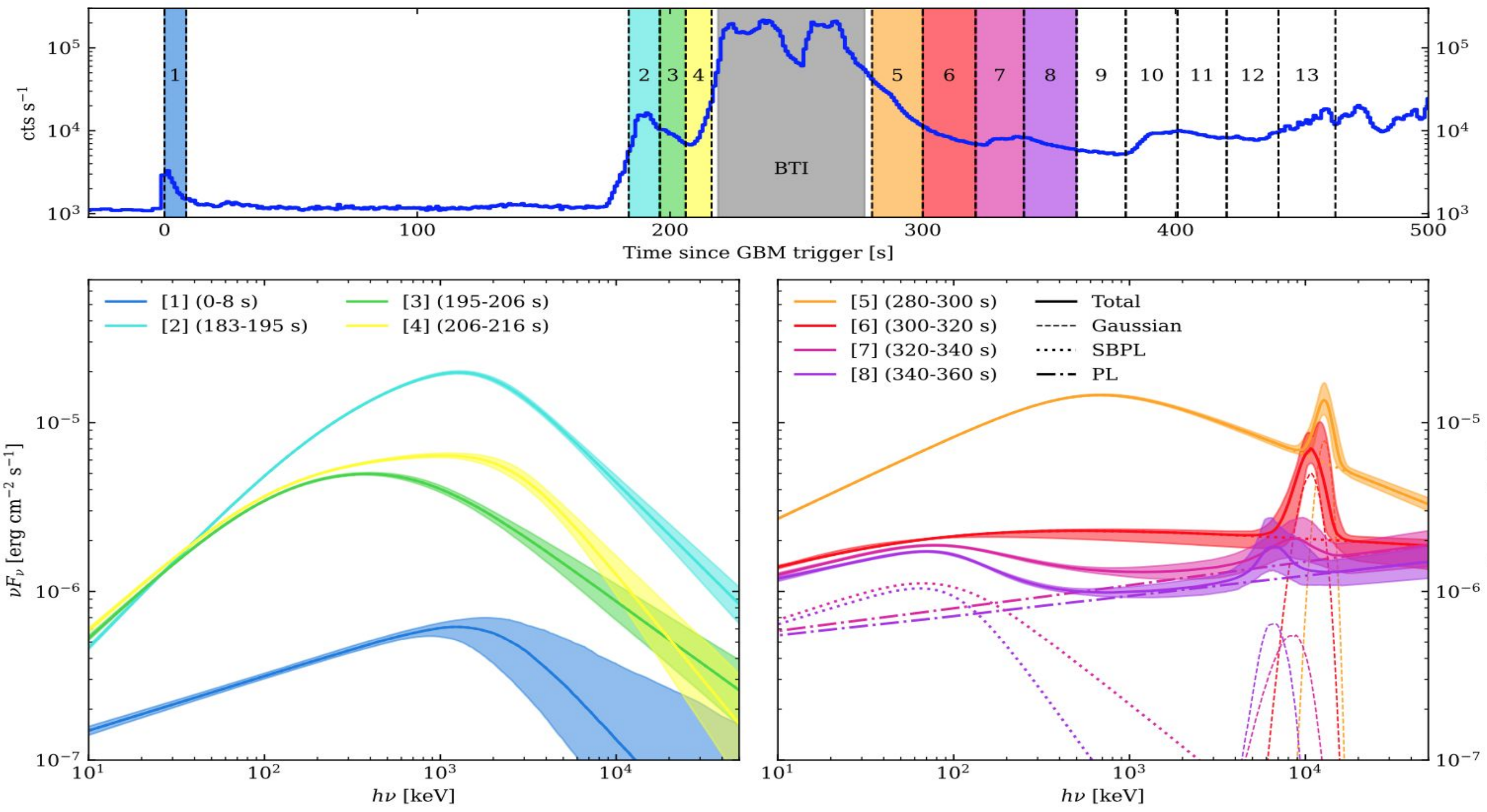

1
2
3
4
BTI
5
6
7
8
9
10
11
12
13
cts s^{-1}
Time since GBM trigger [s]
[1] (0-8 s)
[2] (183-195 s)
[3] (195-206 s)
[4] (206-216 s)
[5] (280-300 s)
[6] (300-320 s)
[7] (320-340 s)
[8] (340-360 s)
Total
Gaussian
SBPL
PL
νF_ν [erg cm^{-2} s^{-1}]
$h\nu$ [keV]

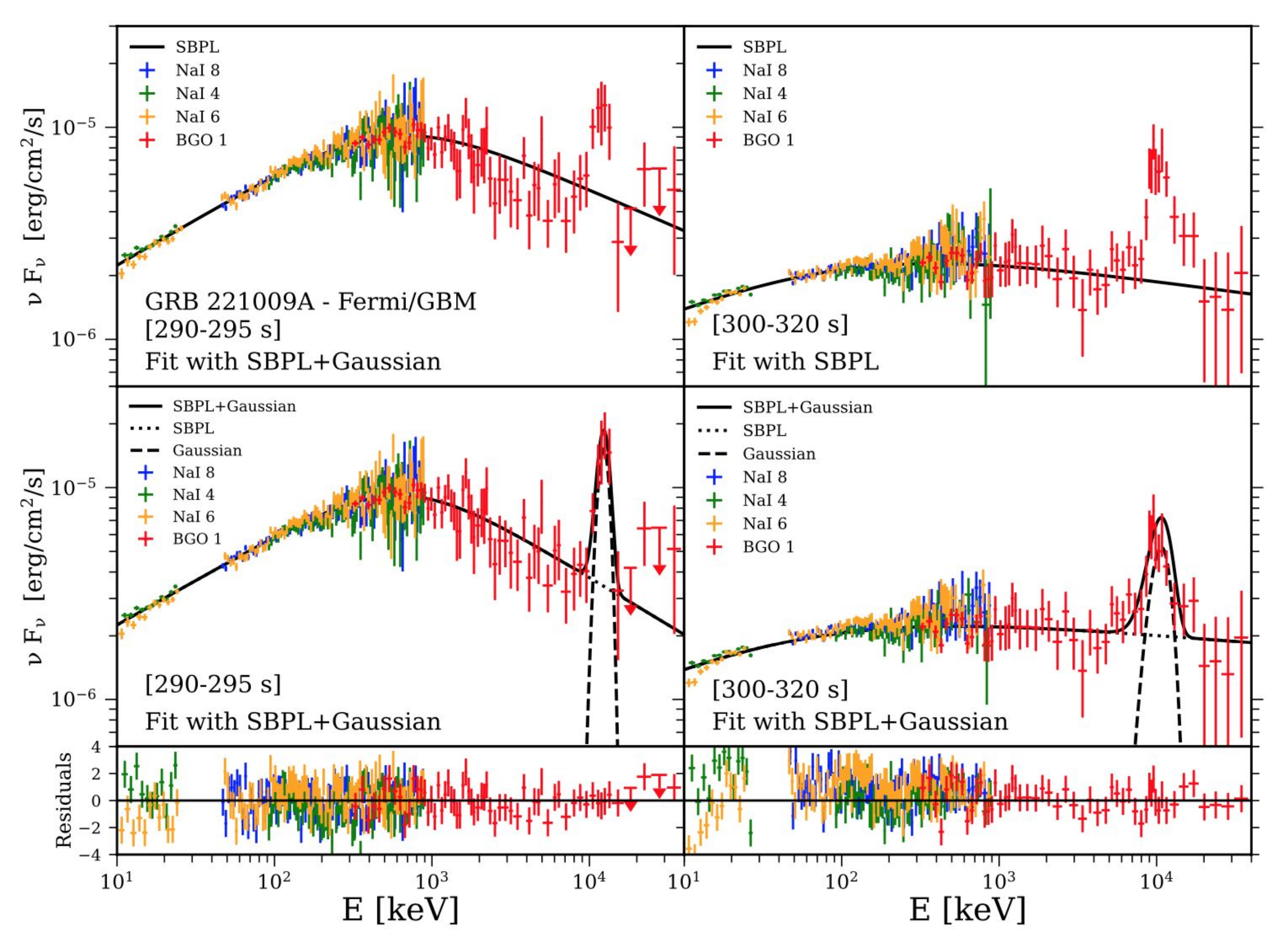

GRB 221009A - Fermi/GBM
[290-295 s]
Fit with SBPL+Gaussian
[300-320 s]
Fit with SBPL
[290-295 s]
Fit with SBPL+Gaussian
[300-320 s]
Fit with SBPL+Gaussian
SBPL
SBPL+Gaussian
Gaussian
NaI 8
NaI 4
NaI 6
BGO 1
νF_ν [erg/cm^2/s]
Residuals
E [keV]

Time interval [s]	L_{gauss} [10^{50} erg/s]	E_{gauss} [MeV]	σ_{gauss} [MeV]	ΔAIC
280 - 300 [5]	$1.12^{+0.19}_{-0.19}$	$12.56^{+0.30}_{-0.31}$	$1.31^{+0.31}_{-0.30}$	49
280 - 285 [5.1]	$0.77^{+0.42}_{-0.42}$	$14.40^{+0.86}_{-0.87}$	$0.99^{+0.66}_{-0.57}$	2.4
285 - 290 [5.2]	$0.43^{+0.33}_{-0.28}$	$13.21^{+6.36}_{-1.51}$	$1.14^{+0.59}_{-0.62}$	-1.2
290 - 295 [5.3]	$1.84^{+0.36}_{-0.33}$	$12.16^{+0.30}_{-0.30}$	$1.08^{+0.34}_{-0.30}$	42
295 - 300 [5.4]	$0.63^{+0.28}_{-0.27}$	$12.55^{+0.47}_{-1.45}$	$0.79^{+0.81}_{-0.45}$	5
300 - 320 [6]	$1.14^{+0.20}_{-0.18}$	$10.19^{+0.29}_{-0.28}$	$1.70^{+0.52}_{-0.42}$	141
300 - 310 [6.1]	$1.08^{+0.19}_{-0.17}$	$10.42^{+0.31}_{-0.30}$	$1.14^{+0.36}_{-0.29}$	45
310 - 320 [6.2][1]	$0.75^{+0.21}_{-0.19}$	$9.77^{+0.42}_{-0.49}$	$1.24^{+0.25}_{-0.21}$	30
320 - 340 [7][1]	$0.23^{+0.15}_{-0.13}$	$7.22^{+1.63}_{-1.72}$	$2.38^{+0.45}_{-0.83}$	-2
340 - 360 [8][1]	$0.21^{+0.12}_{-0.10}$	$6.12^{+0.74}_{-0.59}$	$1.35^{+1.08}_{-0.74}$	0

[1]These spectra require the presence of an extra power-law component.

Time interval [s]	L_{gauss} [10^{50} erg/s]	E_{gauss} [MeV]	σ_{gauss} [MeV]	ΔAIC
280 - 300 [5]	$1.12^{+0.19}_{-0.19}$	$12.56^{+0.30}_{-0.31}$	$1.31^{+0.31}_{-0.30}$	49
280 - 285 [5.1]	$0.77^{+0.42}_{-0.42}$	$14.40^{+0.86}_{-0.87}$	$0.99^{+0.66}_{-0.57}$	2.4
285 - 290 [5.2]	$0.43^{+0.33}_{-0.28}$	$13.21^{+6.36}_{-1.51}$	$1.14^{+0.59}_{-0.62}$	-1.2
290 - 295 [5.3]	$1.84^{+0.36}_{-0.33}$	$12.16^{+0.30}_{-0.30}$	$1.08^{+0.34}_{-0.30}$	42
295 - 300 [5.4]	$0.63^{+0.28}_{-0.27}$	$12.55^{+0.47}_{-1.45}$	$0.79^{+0.81}_{-0.45}$	5
300 - 320 [6]	$1.14^{+0.20}_{-0.18}$	$10.19^{+0.29}_{-0.28}$	$1.70^{+0.52}_{-0.42}$	141
300 - 310 [6.1]	$1.08^{+0.19}_{-0.17}$	$10.42^{+0.31}_{-0.30}$	$1.14^{+0.36}_{-0.29}$	45
310 - 320 [6.2][1]	$0.75^{+0.21}_{-0.19}$	$9.77^{+0.42}_{-0.49}$	$1.24^{+0.25}_{-0.21}$	30
320 - 340 [7][1]	$0.23^{+0.15}_{-0.13}$	$7.22^{+1.63}_{-1.72}$	$2.38^{+0.45}_{-0.83}$	-2
340 - 360 [8][1]	$0.21^{+0.12}_{-0.10}$	$6.12^{+0.74}_{-0.59}$	$1.35^{+1.08}_{-0.74}$	0

[1]These spectra require the presence of an extra power-law component.

Time interval [s]	L_{gauss} [10^{50} erg/s]	E_{gauss} [MeV]	σ_{gauss} [MeV]	ΔAIC
280 - 300 [5]	$\boxed{1.12^{+0.19}_{-0.19}}$	$\boxed{12.56^{+0.30}_{-0.31}}$	$1.31^{+0.31}_{-0.30}$	49
280 - 285 [5.1]	$0.77^{+0.42}_{-0.42}$	$14.40^{+0.86}_{-0.87}$	$0.99^{+0.66}_{-0.57}$	2.4
285 - 290 [5.2]	$0.43^{+0.33}_{-0.28}$	$13.21^{+6.36}_{-1.51}$	$1.14^{+0.59}_{-0.62}$	-1.2
290 - 295 [5.3]	$1.84^{+0.36}_{-0.33}$	$12.16^{+0.30}_{-0.30}$	$1.08^{+0.34}_{-0.30}$	42
295 - 300 [5.4]	$0.63^{+0.28}_{-0.27}$	$12.55^{+0.47}_{-1.45}$	$0.79^{+0.81}_{-0.45}$	5
300 - 320 [6]	$1.14^{+0.20}_{-0.18}$	$10.19^{+0.29}_{-0.28}$	$1.70^{+0.52}_{-0.42}$	141
300 - 310 [6.1]	$1.08^{+0.19}_{-0.17}$	$10.42^{+0.31}_{-0.30}$	$1.14^{+0.36}_{-0.29}$	45
310 - 320 [6.2][1]	$0.75^{+0.21}_{-0.19}$	$9.77^{+0.42}_{-0.49}$	$1.24^{+0.25}_{-0.21}$	30
320 - 340 [7][1]	$0.23^{+0.15}_{-0.13}$	$7.22^{+1.63}_{-1.72}$	$2.38^{+0.45}_{-0.83}$	-2
340 - 360 [8][1]	$\boxed{0.21^{+0.12}_{-0.10}}$	$\boxed{6.12^{+0.74}_{-0.59}}$	$1.35^{+1.08}_{-0.74}$	0

[1]These spectra require the presence of an extra power-law component.

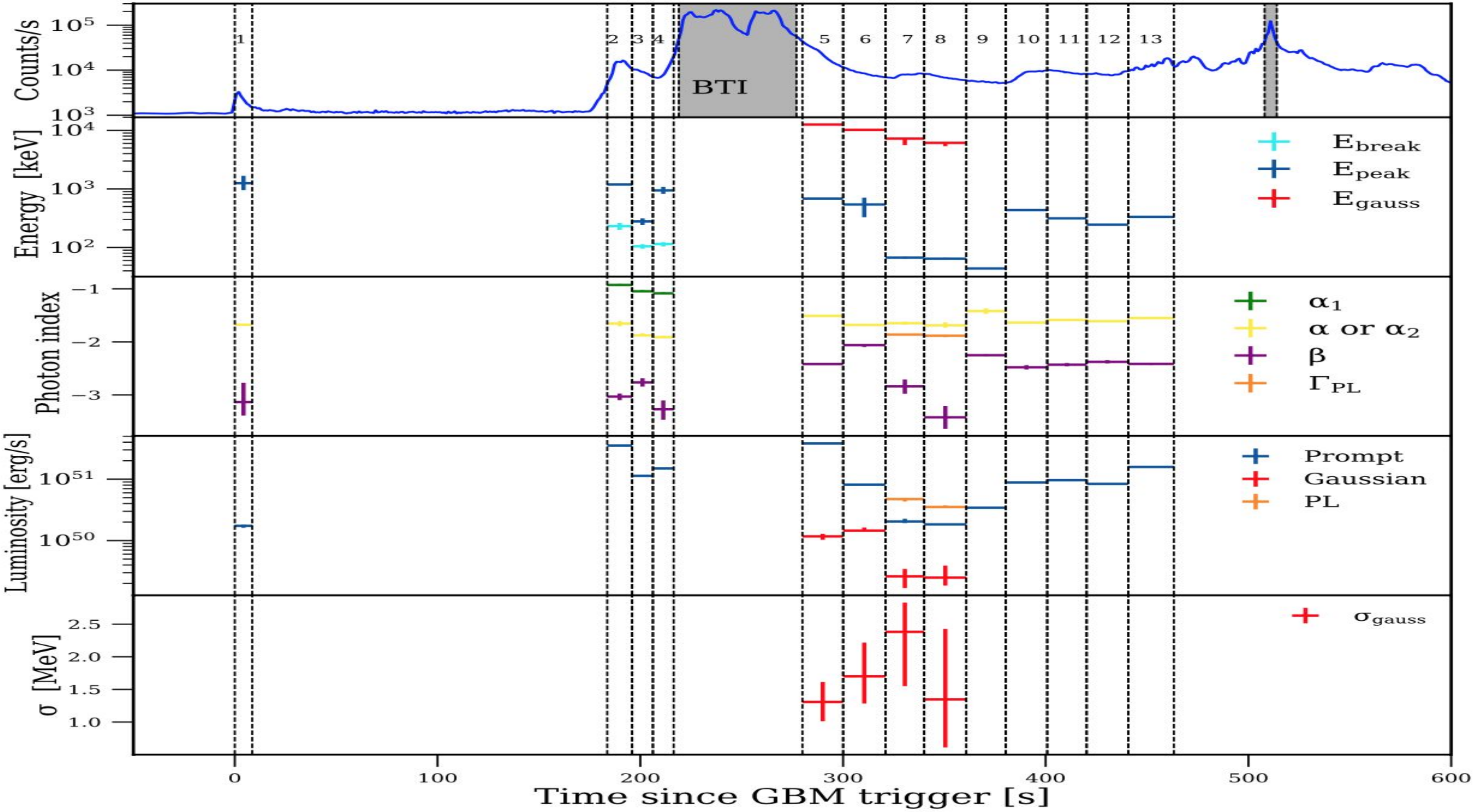

Counts/s
BTI
1 2 3 4 5 6 7 8 9 10 11 12 13
Energy [keV]
E_{break}
E_{peak}
E_{gauss}
Photon index
α_1
α or α_2
β
Γ_{PL}
Luminosity [erg/s]
Prompt
Gaussian
PL
σ [MeV]
σ_{gauss}
Time since GBM trigger [s]

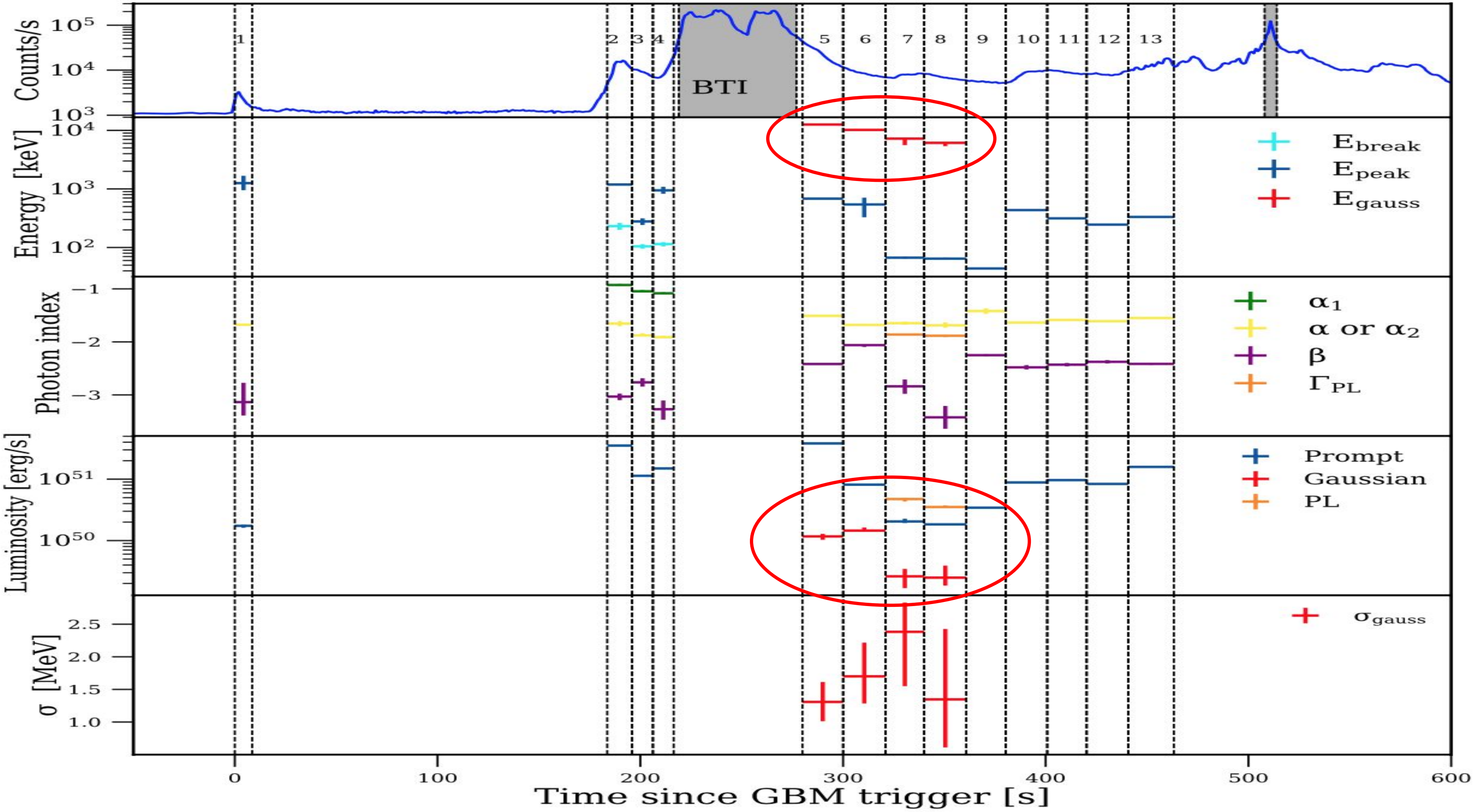

Counts/s
BTI
1
2
3
4
5
6
7
8
9
10
11
12
13
Energy [keV]
E_{break}
E_{peak}
E_{gauss}
Photon index
α_1
α or α_2
β
Γ_{PL}
Luminosity [erg/s]
Prompt
Gaussian
PL
σ [MeV]
σ_{gauss}
Time since GBM trigger [s]

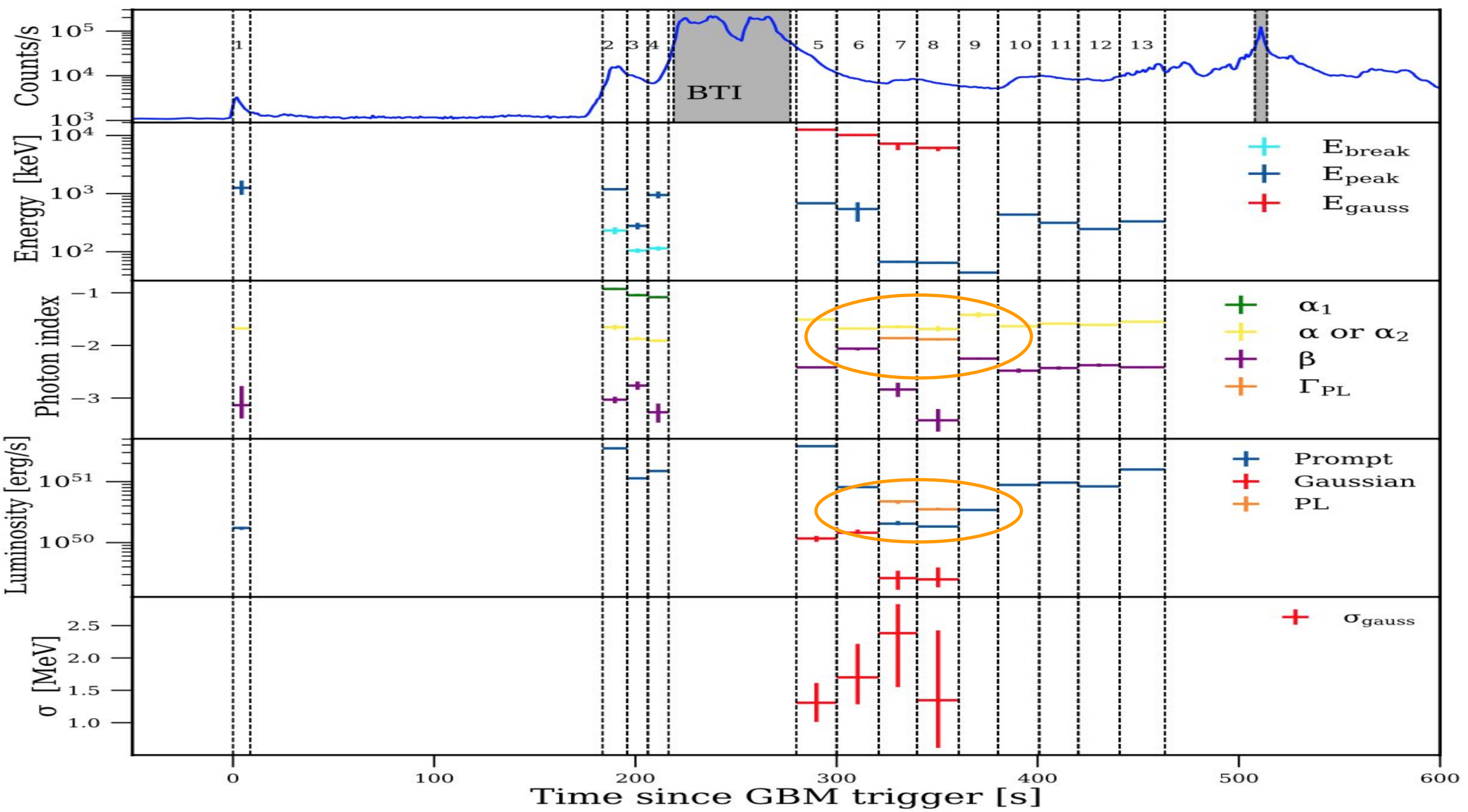

Counts/s
Energy [keV]
Photon index
Luminosity [erg/s]
σ [MeV]
BTI
1
2
3
4
5
6
7
8
9
10
11
12
13
E_break
E_peak
E_gauss
α_1
α or α_2
β
Γ_PL
Prompt
Gaussian
PL
σ_gauss
Time since GBM trigger [s]

Possible scenarios:

- Low energy spectral line (e.g. fluorescent K-α iron line) from "narrow line region" (supernova ejecta) up-scattered by relativistic jet.
    - Radius for the narrow line region ≥ jet photospheric radius -> high Lorentz factor of SN ejecta
    - Low Lorentz factor ($\Gamma \sim 40$) at photosphere
- High-latitude emission (HLE) from shell that produced the most luminous pulse.
    - HLE would affect the entire prompt spectrum -> the line should not be visible.
- **(blue shifted) annihilation line of $e^+ e^-$** (expected in the internal shock scenario)

Controls:

- **Potential instrument effects**
    - Not consider the BTI
    - Background

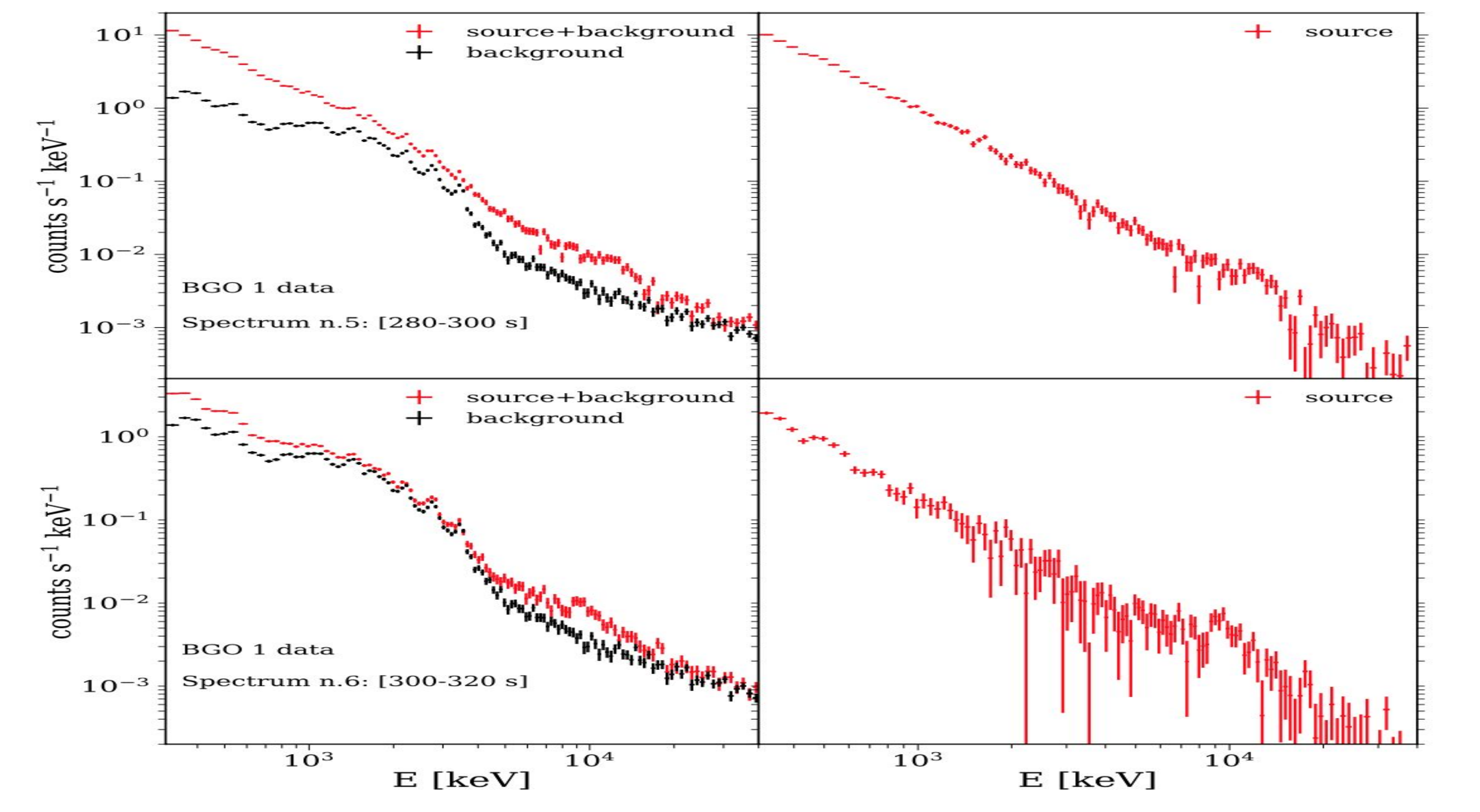

source+background
background
BGO 1 data
Spectrum n.5: [280-300 s]
source
source+background
background
BGO 1 data
Spectrum n.6: [300-320 s]
source
counts s^{-1} keV^{-1}
E [keV]

Controls:

- **Potential instrument effects**
  - Not consider the BTI
  - Background
  - Consider both the BGO detectors

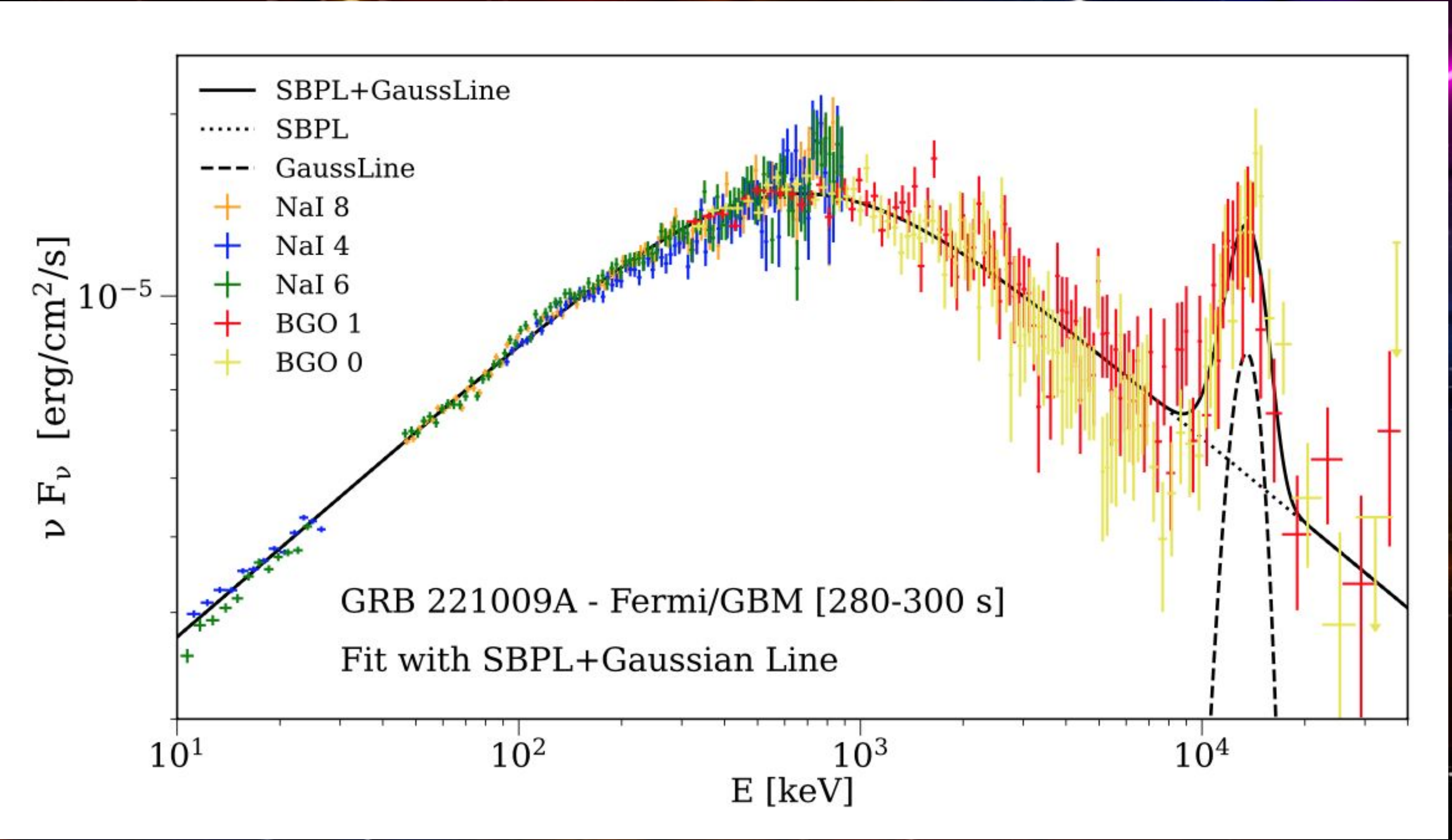

SBPL+GaussLine
SBPL
GaussLine
NaI 8
NaI 4
NaI 6
BGO 1
BGO 0
νF_ν [erg/cm^2/s]
10^{-5}
10^1
10^2
10^3
10^4
E [keV]
GRB 221009A - Fermi/GBM [280-300 s]
Fit with SBPL+Gaussian Line

Controls:

- **Potential instrument effects**
    - Not consider the BTI
    - Background
    - Consider both the BGO detectors
- **Comparison with other GRBs**

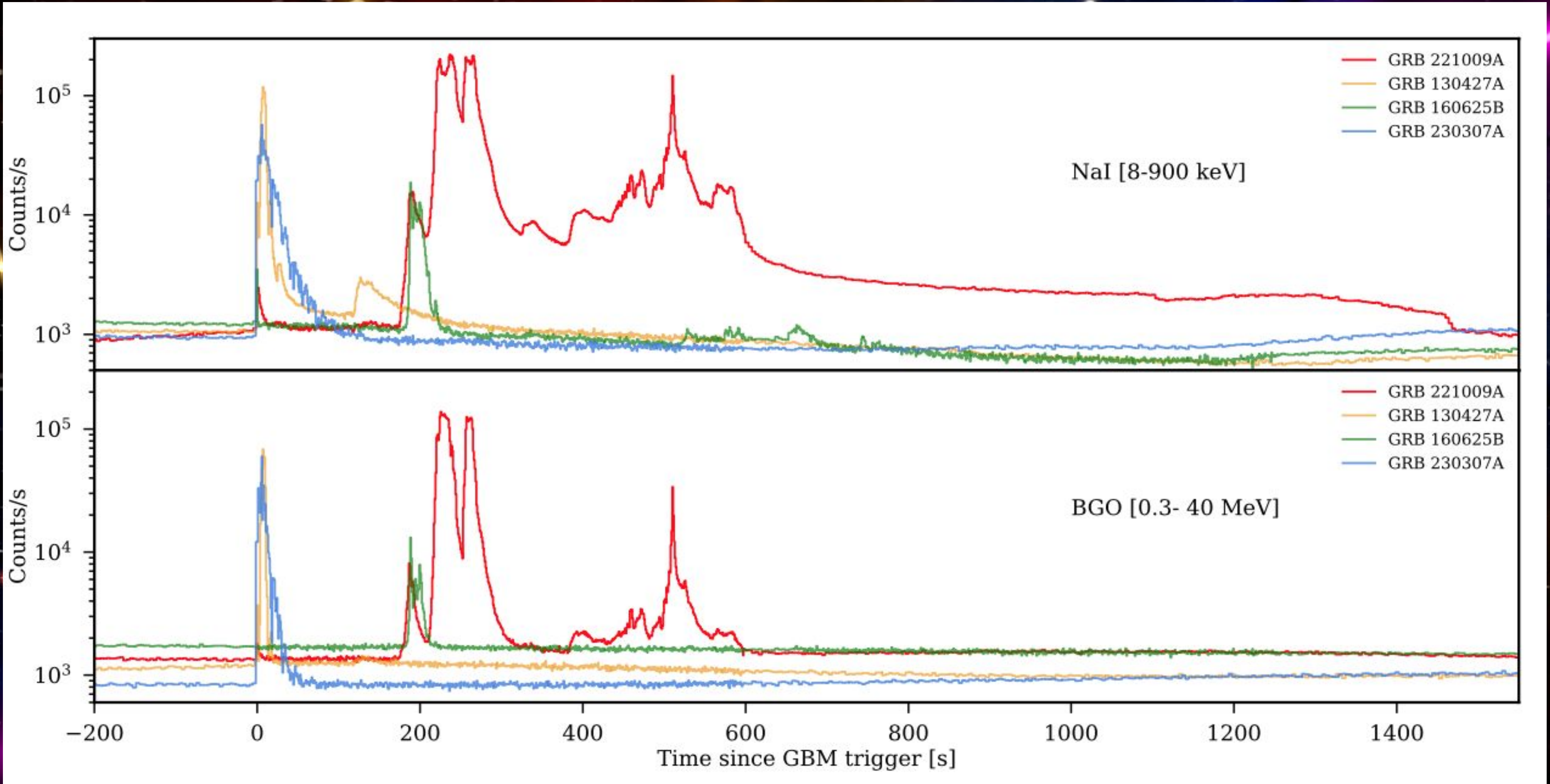

GRB 221009A
GRB 130427A
GRB 160625B
GRB 230307A
NaI [8-900 keV]
Counts/s
10^5
10^4
10^3
GRB 221009A
GRB 130427A
GRB 160625B
GRB 230307A
BGO [0.3- 40 MeV]
Counts/s
10^5
10^4
10^3
−200
0
200
400
600
800
1000
1200
1400
Time since GBM trigger [s]

Controls:

- **Potential instrument effects**
  - Not consider the BTI
  - Background
  - Consider both the BGO detectors
- **Comparison with other GRBs**
  - Other papers: **Lesage et al., arXiv:2303.14172**

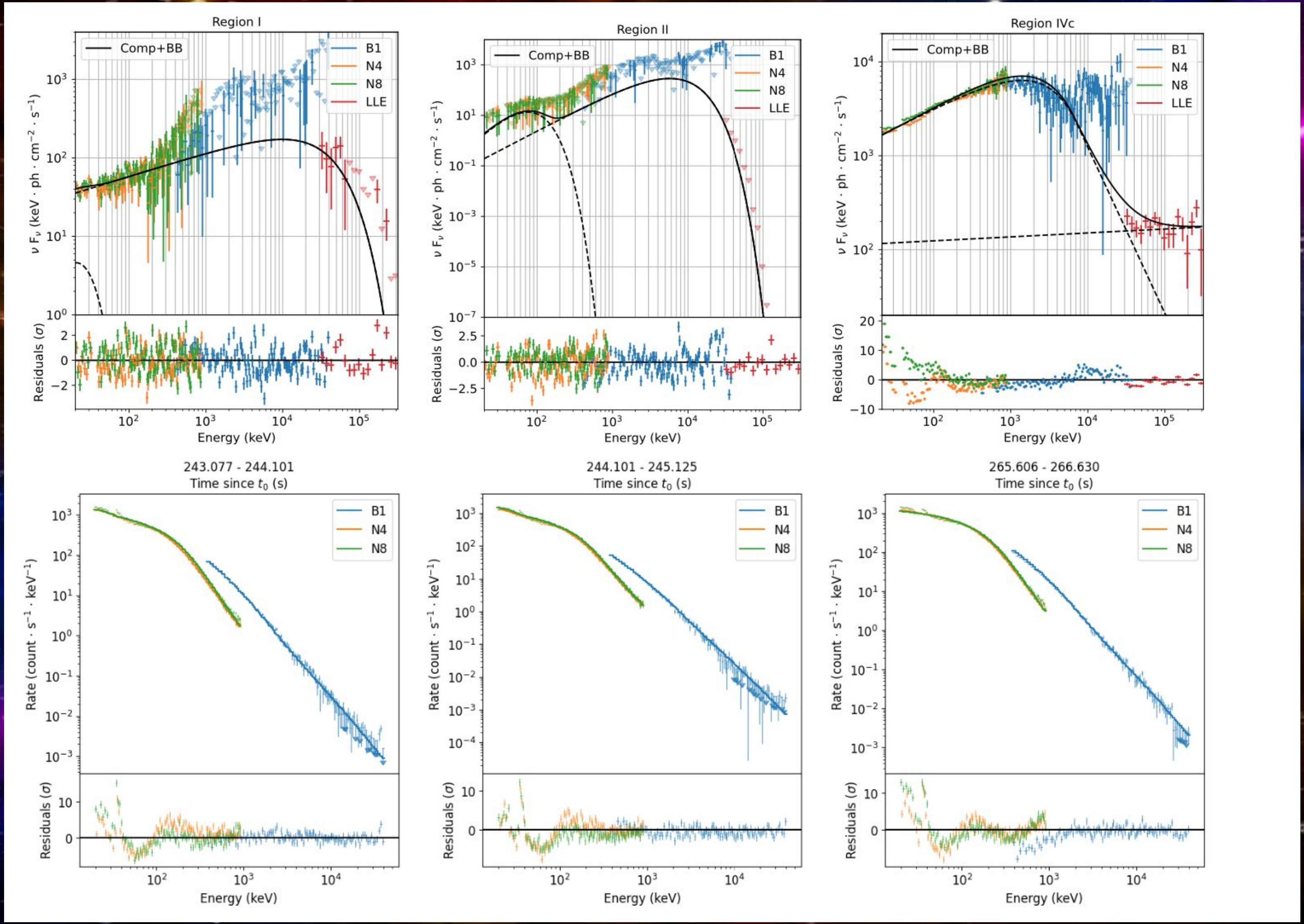
Region I
Region II
Region IVc
Comp+BB
B1
N4
N8
LLE
ν F_ν (keV · ph · cm⁻² · s⁻¹)
Residuals (σ)
Energy (keV)
243.077 - 244.101
244.101 - 245.125
265.606 - 266.630
Time since t₀ (s)
Rate (count · s⁻¹ · keV⁻¹)

Controls:

- **Potential instrument effects**
    - Not consider the BTI
    - Background
    - Consider both the BGO detectors
- **Comparison with other GRBs**
    - Other papers: **Lesage et al., arXiv:2303.14172**
- **Simulations**

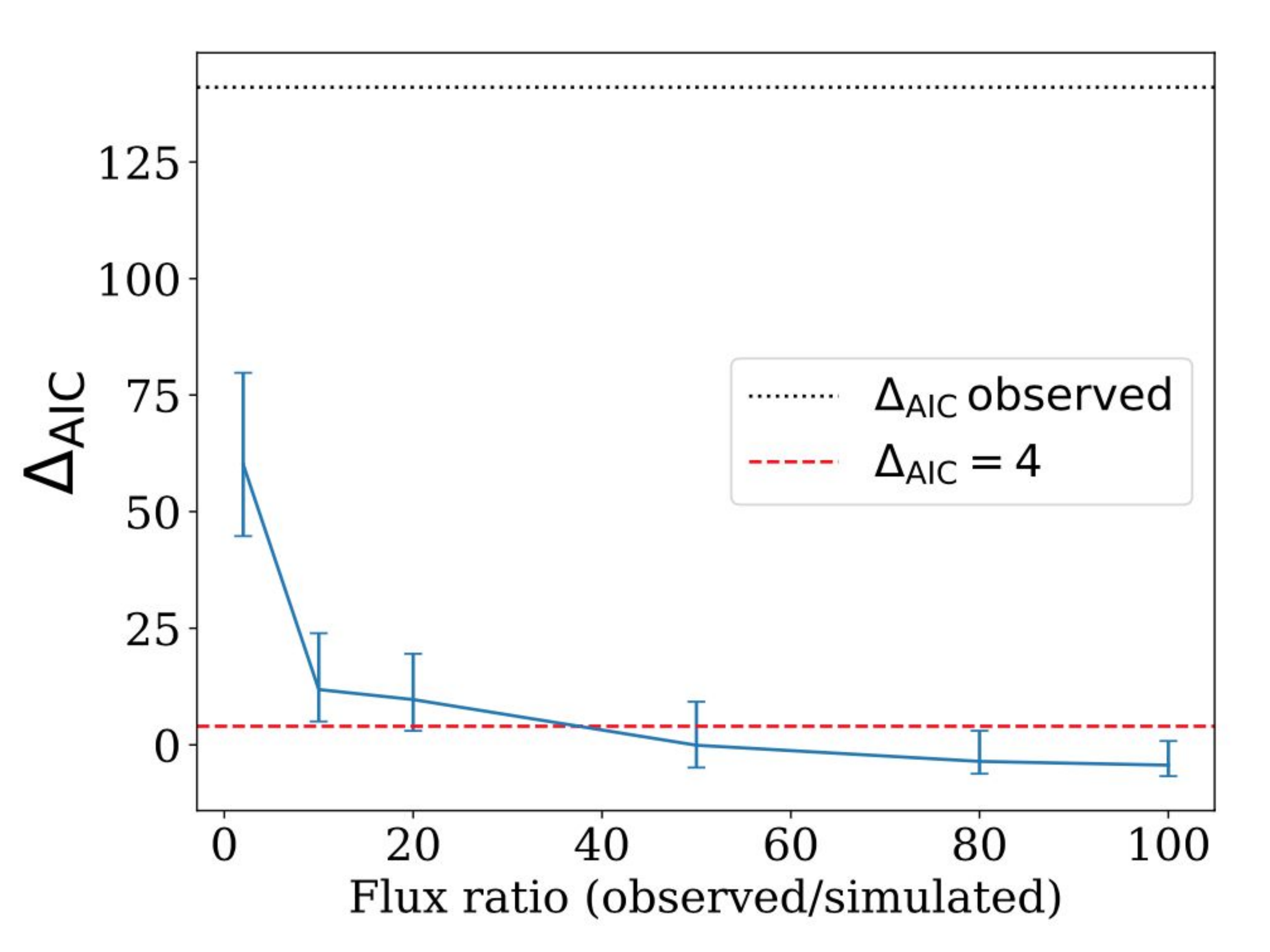

125
100
75
50
25
0
0
20
40
60
80
100
Δ_{AIC}
Flux ratio (observed/simulated)
Δ_{AIC} observed
$\Delta_{AIC} = 4$


Thank you!

Extra slides